WISP Dark Matter eXperiment and Prospects for Broadband Dark Matter Searches in the 1 μeV– 10 meV Mass Range

Dieter Horns[1], Axel Lindner[2], Andrei Lobanov[3,1,†], Andreas Ringwald[2]

[1]Institut für Experimentalphysik, Universität Hamburg, Germany
[2]Deutsches Elektronen-Synchrotron (DESY), Hamburg, Germany
[3]Max-Planck-Institut für Radioastronomie, Bonn, Germany
[†]corresponding author.

Light cold dark matter consisting of weakly interacting slim (or sub-eV) particles (WISPs) has been in the focus of a large number of studies made over the past two decades. The QCD axion and axion-like particles with masses in the $0.1\,\mu eV$–$100\,meV$ are strong candidates for the dark matter particle, together with hidden photons with masses below $\lesssim 100\,meV$. This motivates several new initiatives in the field, including the WISP Dark Matter eXperiment (WISPDMX) and novel conceptual approaches for broad-band WISP searches using radiometry measurements in large volume chambers. First results and future prospects for these experiments are discussed in this contribution.

1 WISP dark matter searches in the 1 μeV–10 meV mass range

Searches for light cold dark matter (DM) consisting of weakly interacting slim particles (WISPs) [1, 2, 3, 4] are gaining prominence, with a number of experiments conducted and proposed detecting hidden photons (HPs), QCD axions, and axion-like particles (ALPs) with astrophysical [5, 6, 7, 8, 9, 10, 11] and laboratory measurements [12, 13, 14, 15, 16, 17].

Best revealed by their coupling to standard model (SM) photons, WISPs can be nonthermally produced in the early Universe [18] and may give rise to dark matter for a broad range of the particle mass and the photon coupling strength [19, 20]. The photon coupling of axions/ALPs, $g_{a\gamma} \propto 1/f_a$, depends on the energy scale f_a of the symmetry breaking responsible for the given particle, while the hidden photon coupling, $\chi \propto g_h$, is determined by the hidden gauge coupling, g_h [19].

At particle masses above $\sim 10^{-3}\,eV$, the existing constraints effectively rule out WISPs as DM particles, while cosmologically viable lower ranges of particle reach down to $\sim 10^{-6}$–$10^{-7}\,eV$ for axions/ALPs and may extend to much lower masses with for HP and ALP, as well as with "fine tuning" of the axion models. The mass range 10^{-7}–$10^{-3}\,eV$ corresponds to the radio regime at frequencies of $24\,MHz$–$240\,GHz$ where highly sensitive measurement techniques are developed for radioastronomical measurements, with typical detection levels of $\lesssim 10^{-22}\,W$.

2 Narrowband experiments

The most sensitive laboratory HP and axion/ALP DM searches performed so far in the mass range 10^{-7}–10^{-3} eV have utilised the "haloscope" approach [21] which employs resonant microwave cavities lowering substantially the detection threshold in a narrow band around each of the cavity resonances [12, 13, 14, 22, 23, 24]. The WISP DM signal results from conversion of DM halo particles inside the cavity volume, V, into normal photons. This conversion is achieved via spontaneous kinetic mixing of HP with SM photons or via the Primakov process induced by an external magnetic field, $\mathbf{B}$, for axions/ALPs.

The output power of the axion/ALP conversion signal is $P_{\mathrm{out}} \propto G\,Q\,V\,|\mathbf{B}|^2$, where Q is the resonant enhancement factor (quality factor) of microwave cavity and G is the fraction of cavity volume (form factor) in which the electric field of the converted photon can be detected [25, 26]. Both G and Q depend on the cavity design and the resonant mode employed in the measurement. The respective P_{out} for the HP signal does not have a dependence on $\mathbf{B}$.

The fractional bandwidth of a haloscope measurement is $\propto Q^{-1}$, with typical values of Q not exceeding $\sim 10^5$. The WISP DM signal itself is restricted to within a fractional bandwidth of $Q_{\mathrm{DM}}^{-1} \approx \sigma_{\mathrm{DM}}^2/c^2 \approx 10^{-6}$, with σ_{DM} describing the velocity dispersion of the dark matter halo. A measurement made at a frequency, ν, and lasting for a time, t, can detect the WISP signal at an SNR $\propto \sqrt{t\,/\,W}\,P_{\mathrm{out}}/(k_{\mathrm{b}}\,T_{\mathrm{n}})$, where W is the signal bandwidth, T_{n} is the noise temperature of the detector, and k_{b} is the Boltzmann constant.

The exceptional sensitivity of microwave cavity experiments comes at the expense of rather low scanning speeds of $\lesssim 1\,\mathrm{GHz/year}$ [12, 27], which makes it difficult to implement this kind of measurements for scanning over large ranges of particle mass. To overcome this difficulty, new experimental concepts are being developed that could relax the necessity of using the resonant enhancement and working in a radiometer mode with an effective $Q = 1$ [16, 17, 28, 29, 30].

2.1 WISP Dark Matter eXperiment

At frequencies below $1\,\mathrm{GHz}$, the ADMX experiment[12, 13, 14] has employed the haloscope approach to probe the HP and axion/ALP dark matter in the 460–860 MHz (1.9–3.6 μeV) range [31], and a high frequency extension, ADMX-HF is planned for he 4–40 GHz frequency range [32, 33]. The WISP Dark Matter eXperiment (WISPDMX, Fig. 1) extends the haloscope searches to particle masses below 1.9 μeV, aiming to cover the range 200–600 MHz (0.8–2.5 μeV).

WISPDMX utilises a 208 MHz resonant cavity of the type used at the proton accelerator ring of the DESY HERA collider [34]. The cavity has a volume of 460 liters and a nominal resonant amplification factor $Q = 55000$ at the ground TM$_{010}$ mode. The signal is amplified by a broad-band 0.2–1 GHz amplifier chain with a total gain of 40 dB. Broad-band digitization and FFT analysis of the signal are performed using a commercial 12-bit spectral analyzer, enabling simultaneous measurements at several resonant modes at frequencies of up to 600 MHz.

The main specific aspects of WISPDMX measurements are: 1) broadband recording in the 200–600 MHz band at a resolution of $\leq 150\,\mathrm{Hz}$, 2) the use of multiple resonant modes tuned by a plunger assembly consisting of two plungers, and 3) the planned use of rotation of the cavity in the magnetic field in order to enable axion measurements at multiple resonant modes as well.

The WISPDMX measurements are split into three different stages: 1) HP DM searches at the nominal frequencies of the resonant modes of the HERA cavity; 2) HP DM searches with cavity tuning (covering up to 70% of the 200–600 MHz band); and 3) axion/ALP DM searches using the DESY H1 solenoid magnet which provides $B = 1.15\,\mathrm{T}$ in a volume of $7.2\,\mathrm{m}^3$.
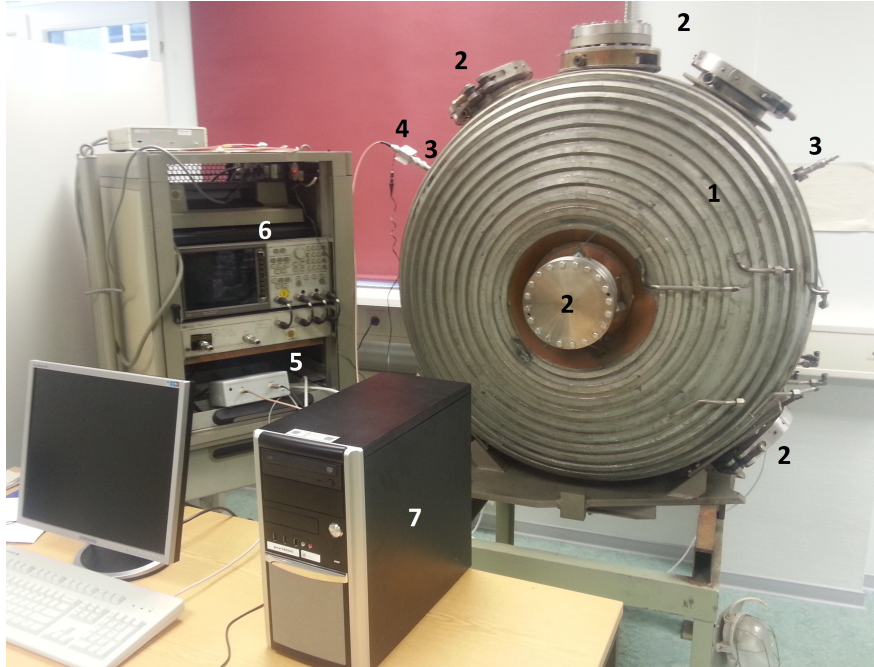
Figure 1: WISPDMX setup for the initial measurements made at nominal resonant frequencies of the microwave cavity. Indicated with numbers are: 1 – a 208-MHz microwave cavity of the type used in the proton ring of the DESY HERA collider; 2 - cavity ports (two on the axis of the cavity and five on the radial wall of the oblate cylinder; 3 – antenna ports for two magnetic-loop antennas inserted in the cavity; 4 – first stage amplifier (WantCom, 0.1-1.0 GHz, 22.5 dB gain, 0.6 dB noise figure); 5 – second stage amplifier (MITEQ, 0.1-0.9 GHz, 18.2 gain, 1.0 dB noise figure); 6 – network analyzer (HP 85047A); 7 – control computer, with a 12-bit digitizer Alazar ATS-9360 operated via a PCIe Gen2 interface.

The first phase of the WISPDMX measurements has been completed [15], and the final results are being prepared for publication. The WISPDMX setup used for these measurements is shown in Fig. 1. Table 2.1 lists preliminary exclusion limits obtained for five different resonant modes of the cavity. These limits reach below $\chi = 3 \times 10^{-12}$ at all of the modes used in the measurement, and already these limits probe the parameter space admitting HP DM. The expected exclusion limits for the HP and axion/ALP DM searches in the next two phases of WISPDMX are shown in Figs. 2-3.

3   Broadband experiments

The relatively low scanning speed (*e.g.*, $\approx 100\,\mathrm{MHz/yr}$ for WISPDMX and $\sim 1\,\mathrm{GHz/yr}$ for ADMX) and limited tunability of resonant experiments make them difficult to be used for covering the entire $1\,\mu\mathrm{eV}$–$10\,\mathrm{meV}$ range of particle mass. The gain in sensitivity provided by the resonant enhancement, Q, needs to be factored against the bandwidth reduction of the

Table 1: WISPDMX measurements at nominal resonant modes in the 200-600 MHz range

Mode	ν [MHz]	Q	$\mathcal{G}$	P_{det} [$\times 10^{-14}$W]	$m_{\gamma_{\text{s}}}$ [μeV]	χ [$\times 10^{-13}$]
TM$_{010}$	207.87961	55405	0.429	1.08	0.85972093	17.0
TE$_{111}$	321.45113	59770	0.674	1.08	1.3294150	8.4
TE$_{111}$	322.74845	58900	0.671	1.08	1.3347803	8.5
TM$_{020}$	454.42411	44340	0.317	1.08	1.8793470	10.1
TE$_{112}$	510.62681	71597	0.020	1.09	2.1117827	28.2
TE$_{112}$	515.97110	67840	0.019	1.09	2.1338849	29.5
TE$_{120}$	577.59175	60350	0.036	1.10	2.3887274	20.4
TE$_{120}$	579.25126	66520	0.037	1.10	2.3955906	19.1

Column designation: resonant mode of the cavity, with its respective resonant frequency, ν, quality factor, Q, geometrical form factor, $\mathcal{G}$, measured noise power, P_{det}, hidden photon mass, $m_{\gamma_{\text{s}}}$, and 95% exclusion limit, χ, for hidden photon coupling to normal photons, calculated for the antenna coupling $\kappa = 0.01$ [15].

order of Q^{-1}, which may result in a somewhat counterintuitive conclusion that non-resonant, broadband approaches may be preferred when dealing with a mass range spanning over several decades.

Indeed, for axion/ALP searches, reaching a desired sensitivity to the photon coupling implies a measurement time $t \propto T_{\text{sys}}^2 B^{-4} V^{-2} G^{-2} Q^{-2}$. A broadband measurement, with $Q_{\text{b}} \equiv 1$, needs to last Q^2 times longer to reach the same sensitivity. However, the broadband measurement probes the entire mass range at once, while it would require a (potentially very large) number of measurements, $N_{\text{mes}} = 1 + \log(\alpha) / \log[Q/(Q-1)]$, in order to cover a range of particle mass from m_1 to $m_2 = \alpha \, m_1$ (with $\alpha > 1$). Then, the broadband approach would be more efficient in case if $t_{\text{b}} < t_{\text{n}} N_{\text{mes}}$. This corresponds to the following comparison between these two types of measurement:

$$1 + Q \log \alpha > \left(\frac{T_{\text{b}}}{T_{\text{n}}}\right)^2 \left(\frac{B_{\text{b}}}{B_{\text{n}}}\right)^{-4} \left(\frac{V_{\text{b}}}{V_{\text{n}}}\right)^{-2} \left(\frac{G_{\text{b}}}{G_{\text{n}}}\right)^{-2} ,$$

where the subscripts b and n refer to the respective parameters of the broadband and narrowband measurements. For typical experimental settings, one can expect that $T_{\text{b}} \sim 100 \, T_{\text{n}}$, $B_{\text{b}} \sim B_{\text{n}}$, $V_{\text{b}} \sim 100 V_{\text{n}}$, and $G_{\text{b}} \sim 0.01 G_{\text{n}}$. In such conditions, a narrowband experiment with $Q > 10^4 / \log \alpha$ would be less efficient in scanning over the given range of mass. Applied to the entire $0.1 \, \mu$eV–$10 \, $meV range of mass, this condition implies restricting the effective resonance enhancement of narrowband measurements to less than ~ 2000, which effectively disfavors the narrowband approach for addressing such a large range of particle mass.

The measurement bandwidth of radiometry experiments is limited only by the detector technology, with modern detectors employed in radio astronomy routinely providing bandwidths in excess of 1 GHz and spectral resolutions of better than 10^6.

One possibility for a radiometer experiment is to employ a spherical dish reflector that provides a signal enhancement proportional to the area of the reflector [16, 28, 29, 30]. This option is well-suited for making measurements at higher frequencies (shorter wavelengths, λ), as the effective signal enhancement is $\propto A_{\text{dish}}/\lambda^2$, where A_{dish} is the reflecting area [16]. It is therefore expected that this concept would be best applicable at $\lambda \lesssim 1 \, $cm ($\nu \gtrsim 30 \, $GHz).
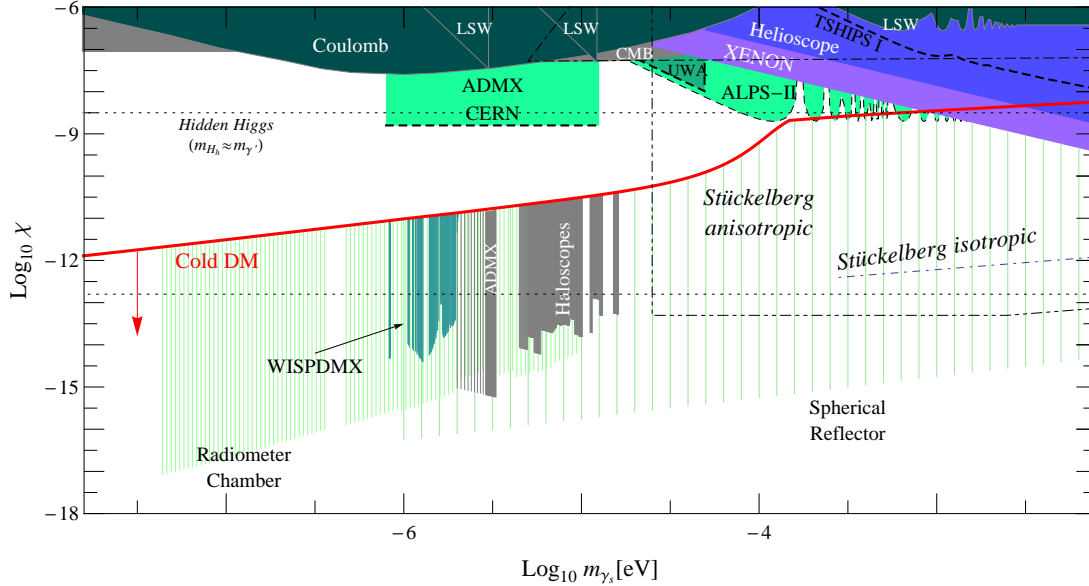
Figure 2: Exclusion limits for hidden photon coupling to normal photons from existing (white captions) and planned (black captions) experiments (adapted from [4]). Theoretical expectations for the hidden photon DM are indicated in red. The expected sensitivity limits of the second phase of the WISPDMX experiment are marked with turquoise color, reaching well into the DM favored range of photon coupling. The WISPDMX sensitivity is calculated for a setup with two tuning plungers operating simultaneously. The hatched areas illustrate the expected sensitivity of broadband experiments using the spherical reflector and the radiometry chamber approaches.

At lower frequencies, another attractive possibility for engaging into the broadband measurements is to use the combination of large chamber volume and strong magnetic field provided by superconducting TOKAMAKs or stellarators such as the Wendelstein 7-X stellarator [35] in Greifswald (providing $B = 3\,T$ in a $30\,m^3$ volume).

3.1 Radiometry chamber experiments

More generally, the stellarator approach signifies a conceptual shift to employing a large, magnetized volume of space which can be probed in a radiometry mode (*radiometer chamber*), without resorting to a resonant enhancement of the signal. The exclusion limits expected to be achievable with the spherical reflector experiments and with the measurements made in a radiometer chamber with the volume and magnetic field similar to those of the Wendelstein stellarator are shown in Fig. 2-3.

Deriving from the stellarator approach, a large chamber can be designed specifically for the radiometer searches, with the inner walls of the chamber covered by multiple fractal antenna elements providing a broad-band receiving response in the 0.1-25 GHz frequency range with a high efficiency and a nearly homogeneous azimuthal receiving pattern [36, 37]. Combination
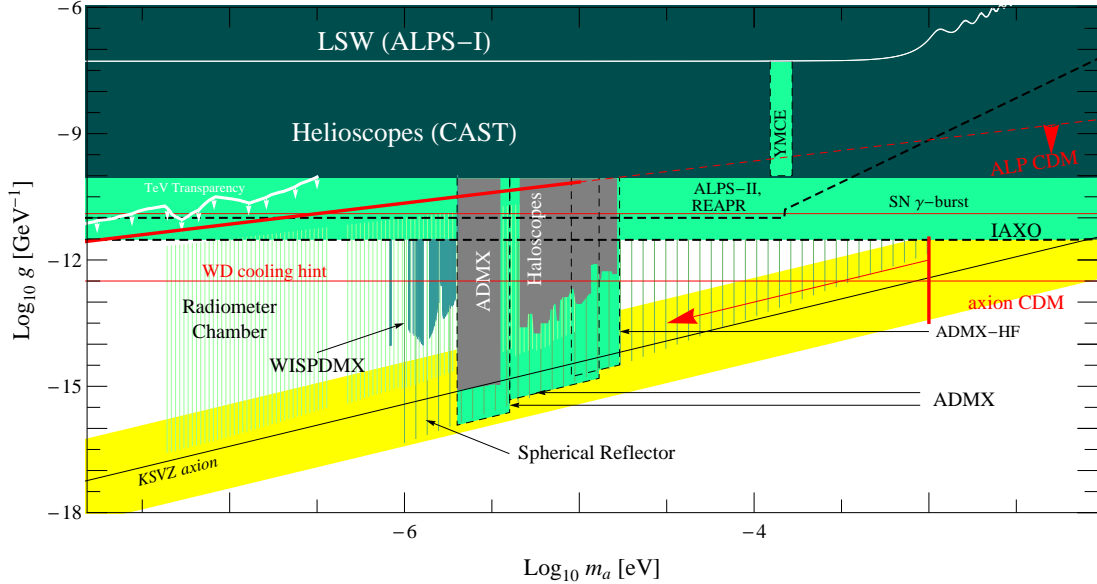
Figure 3: Exclusion limits for axion/ALP photon coupling to normal photons from existing (white captions) and planned (black captions) experiments (adapted from [4]). The yellow band corresponds to the parameter space allowed for the QCD axion. Theoretical expectations for the axion/ALP DM are indicated in red. The expected sensitivity limits of the second phase of the WISPDMX experiment are marked with turquoise color, reaching well into the DM favored range of ALP coupling. The WISPDMX sensitivity is calculated for a setup with two tuning plungers operating simultaneously. The hatched areas illustrate the expected sensitivity of broadband experiments using the spherical reflector and the radiometry chamber approaches.

of multiple receiving elements provides also the possibility for achieve directional sensitivity to the incoming photons.

The directional sensitivity can be realized through high time resolution enabling phase difference measurements between individual fractal antenna elements. Making such measurements is well within the reach of the present day data recording implemented for radio interferometric experiments with the recording rate as high as 16 Gigabit/sec [38]. This recording rate provides a time resolution down to 0.12 nanoseconds, thus enabling phase measurements over effective travel path difference $\delta_l \approx 4$ millimetres. This corresponds to an angular resolution ϕ_p in the range of $R/(L/\delta_l + 1)[(R^2 + L^2)^{1/2} - \delta_l]^{-1} \lesssim \phi_p \lesssim (2R/\delta_l + 1)^{1/2}/(R/\delta_l + 1)$, where R and L denote the smallest and largest dimensions of the chamber, respectively. For a chamber fitted into the HERA H1 magnet (assuming $R \approx 1\,\mathrm{m}$ and $L \approx 3\,\mathrm{m}$), this corresponds to angular resolutions of $0.05° \lesssim \phi_p \lesssim 5°$. The radiometry chamber measurements could therefore provide an attractive experimental concept for performing WISP DM searches in the range of particle mass between 0.1 and $2\,\mu\mathrm{eV}$, thus closing the low end of the parameter space still open for the axion dark matter.

Acknowledgments

References

[1] R. Essig, J. A. Jaros, W. Wester *et al.*, "Dark Sectors and New, Light, Weakly-Coupled Particles", [arXiv:1311.0029 [hep-ph]].

[2] J. Jaeckel and A. Ringwald, Ann. Rev. Nucl. Part. Sci. **60** (2010) 405 [arXiv:1002.0329 [hep-ph]].

[3] A. Ringwald, Phys. Dark Univ. **1**, 116 (2012) [arXiv:1210.5081 [hep-ph]].

[4] J. L. Hewett, H. Weerts, R. Brock *et al.*, arXiv:1205.2671 [hep-ex].

[5] A. Mirizzi, J. Redondo and G. Sigl, JCAP **0903**, 026 (2009) [arXiv:0901.0014 [hep-ph]].

[6] A. Mirizzi, J. Redondo and G. Sigl, JCAP **0908**, 001 (2009) [arXiv:0905.4865 [hep-ph]].

[7] D. Chelouche, R. Rabadán, S.S. Pavlov, F. Castejón, ApJSS **180**, 1 (2009) [arXiv:0806.0411 [astro-ph]].

[8] M.S. Pshirkov, S.B. Popov, JETP **108**, 384 (2009) [arXiv:0711.1264 [astro-ph]].

[9] D. Horns, L. Maccione, A. Mirizzi, M. Roncadelli, Phys. Rev. D **85** 085021 (2012).

[10] D. Horns, M. Meyer, JCAP **2** 33 (2012).

[11] A. P. Lobanov, H.-S. Zechlin, D. Horns, Phys. Rev. D **87**, 065004 (2013) [arXiv:1211.6268 [astro-ph.co]]

[12] R. Bradley, J. Clarke, D. Kinion *et al.*, Rev. Mod. Phys. **75**, 777 (2003).

[13] [ADMX Collaboration], S. J. Asztalos *et al.*, Phys. Rev. Lett. **104**, 041301 (2010) [arXiv:0910.5914 [hep-ex]].

[14] A. Wagner, G. Rybka, M. Hotz *et al.*, Phys. Rev. Lett. **105**, 171801 (2010) [arXiv:1007.3766 [hep-ex]].

[15] S. Baum, *WISPDMX - Eine direkte Suche nach Dunkler Materie mit einer 208 MHz HERA-Kavität*, Universität Hamburg, 2013 (www.iexp.uni-hamburg.de/groups/astroparticle/de/forschung/BA_2013-12-04_final.pdf)

[16] D. Horns, J. Jaeckel, A. Lindner, *et al.*, JCAP **4**, 016 (2013) [arXiv:1212.2970 [hep-ph]].

[17] D. Horns, A. Lindner, A. P. Lobanov, A. Ringwald, Proc. of IX Patras Workshop *(in press)* (2014), [arXiv:1309.4170 [hep-ph]].

[18] Pierre Sikivie, Lect. Notes Phys. **741** 19 (2008), [astro-ph/0610440].

[19] P. Arias, D. Cadamuro, M. Goodsell, *et al.*, JCAP **1206**, 013 (2012) [arXiv:1201.5902 [hep-ph]].

[20] J. Redondo, B. Döbrich, arXiv:1311.5341 [hep-ex].

[21] P. Sikivie, Phys. Rev. Lett. **51** 1415 (1983).

[22] S. De Panfilis *et al.*, Phys. Rev. Lett. **59**, 839 (1987).

[23] W. Wuensch *et al.*, Phys. Rev. **D40**, 3153 (1989).

[24] C. Hagmann, P. Sikivie, N. S. Sullivan, and D. B. Tanner, Phys. Rev. **D42**, 1297 (1990).

[25] S. J. Asztalos *et al.*, Phys. Rev. **D64**, 092003 (2001).

[26] O. K. Baker, M. Betz, F. Caspers, *et al.*, [arXiv:1110.2180 [physics.ins-det]].

[27] C. Hagmann, P. Sikivie, N. Sullivan, D. B. Tanner and S. I. Cho, Rev. Sci. Instrum. **61** 1076 (1990)

[28] J. Jaeckel, J. Redondo, Phys. Rev. D **88** 115002 (2013) [arXiv:1308.1103 [hep-ph]].

[29] J. Jaeckel, J. Redondo, JCAP **11** 16 (2013) [arXiv:1307.7181 [hep-ph]].

[30] B. Döbrich, Proc. of X Patras Workshop *(this volume)* (2015).

[31] S. J. Asztalos, *et al.*, Phys. Rev. Lett. **104** 041301 (2010) [arXiv:0910.5914] [hep-ph]].

[32] K. van Bibber, G. Carosi, [arXiv:1304.7803 [physics.ins-det]] (2013).

[33] L. J. Rosenberg, Proc. of X Patras Workshop *(this volume)* (2015).

[34] A. Gamp, *Particle Accelerators* **29** 65 (1990)

[35] M. Hirsch, J. Baldzuhn, C. Beidler, *et al.*, Plasma Phys. Control. Fusion **50** 053001 (2008).

[36] A. Azari, R. Rowhani, Progr. in Electromag. Res. C **2** 7 (2008).

[37] S. N. Khan, J. Hu, J. Xiong, S. He, Progr. in Electromag. Res. Lett. **1** 19 (2008).

[38] A. R. Whitney, C. J. Beaudoin, R. J. Cappallo, *et al.*, arXiv:1210.5961 (2012).